Non-Ohmic Variable-Range Hopping and Resistive Switching in $SrTiO_3$ Domain Walls

H. J. Harsan Ma[1,2,*] and J. F. Scott[3,†]

[1]Low Dimensional Quantum Physics & Device Group, School of Microelectronics, Xidian University, 2 South Taibai Road, Xi'an 710071, China

[2]State Key Discipline Laboratory of Wide Band Gap Semiconductor Technology, School of Microelectronics, Xidian University, 2 South Taibai Road, Xi'an 710071, China

[3]Schools of Chemistry and Physics, St Andrews University, St. Andrews KY16 9SS, United Kingdom

(Received 14 October 2019; revised manuscript received 4 January 2020; accepted 28 February 2020; published 6 April 2020)

We report observation of electric field driven conductivity with negative differential conductance and resistive switching in insulating $SrTiO_3$ samples over a wide range of applied voltages at low temperatures. The observed current follows $I = I_0 \exp[-(E^*/E)^{1/2}]$ at large applied electric field, corresponding to variable range hopping conduction with a Coulomb gap in domain walls. Our data are sufficient to discriminate unambiguously between Shklovskii and Mott hopping via their different electric field exponent. Under some conditions space-charge-limited currents are observed, and the charge mobility limit is determined to be in the range of 17 and 210 cm^2/Vs.

DOI: 10.1103/PhysRevLett.124.146601

The future development of nanodevices and in particular of ferroics (ferroelectric, ferroelastic, dielectrics) switching memory devices is a high priority now. Much of the research has been focused on the use of naturally occurring domain walls as the conducting interconnects [1,2]. Since conventional metal interconnects take up an increasingly large fraction of device volume as the devices are reduced in size, such naturally occurring conduction paths save space, processing steps, and cost. Ferroelastic or ferroelectric domain walls are extremely narrow (ca. nm, orders of magnitude thinner than magnetic walls), so such devices would be ideal.

Though it has been shown that interface-limited mechanisms dominate conduction in ferroelectric materials [3–5], it is not straightforward to determine a single mechanism especially in bulk-limited conduction responsible for the observed conduction through domain walls. In some cases, *IV* data could be fitted well by different models [5] which could possibly lead to different results. The obtained results are also rather sensitive to the interface or barriers between the used electrodes (including conducting tips which inevitably introduces large barrier potential) and domain walls. It is desirable to study systems with ferroelectric or polar domain walls in the paraelectric domain matrix and minimized influence from electrodes or domain wall barriers or interfaces. Ferroelastic strontium titanate ($SrTiO_3$) with polar and conducting domain walls within insulating domains [6–9] is an ideal platform for such a study. In the present work we show bulk-limited conduction in strontium titanate crystals dominated by Shklovskii variable range hopping at low temperature, and we can unambiguously discriminate Shklovskii hopping from other conduction mechanisms like Mott hopping via their different electric field exponents. Space charge limited currents are also observed, which enables us to determine the mobility limit of the charges.

As a central oxide, $SrTiO_3$ (STO) plays an important role in oxide electronics, both on account of its multifunctional properties and its suitability as a substrate for all-oxide heterostructures. STO undergoes a ferroelastic transition forming tetragonal domains and domain walls below ~105–110 K. We have recently demonstrated that ferroelectric domain walls could be created and induced in STO by applying an external electric field above a threshold of 1.5 kV/cm; in the interim the matrices among domain walls remain paraelectric [10]. STO could be made n-type conducting by growing a top overlayer [11], forming a perfect contact between electrodes (n-type conducting STO induced by overlayer) and insulating bulk (STO and domains therein), as both of them are STO itself with minimized potential difference, unlike the typical metal-oxide contacts (Fig. 1). As the domain walls in STO intersect with each other, optimized conducting channels form between n-type conducting STO and domain walls [Figs. 1(c), 1(d)]. As it remains unclear whether domain walls are heavily semiconducting (due to the presence of impurity bands E_{im}) or metallic (due to the presence of domain wall bands E_{dm}), we schematically show both of them in Fig. 1.

Here we describe the observation of electrical conductivity at domain walls in the prototypical ferroelastic $SrTiO_3$ (STO) by using transport measurement. We use commercial bulk STO single crystals for measuring the conductivity behaviors of the domain walls. Two types of electrodes have been used to measure conductivity of insulating STO, one is gold electrodes [Fig. 1(a)], another

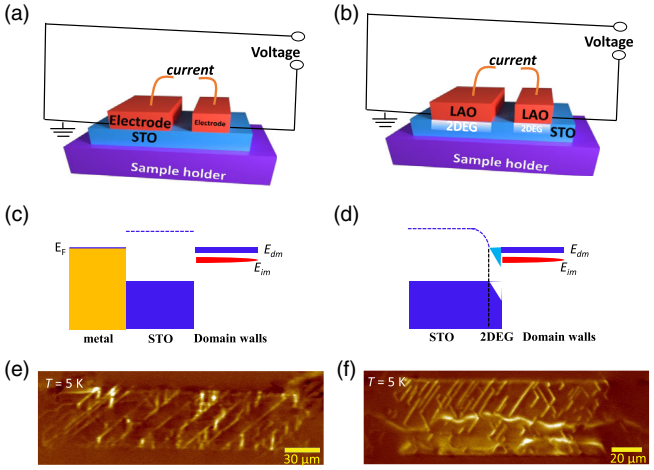

FIG. 1. Experimental setup and ferroelastic or ferroelectric domain walls in STO. Schematic illustration of the transport experimental setup and device scheme by using gold electrodes (a) and conducting n-type STO 2DEG layer induced by LAO (b) on insulating STO. (c),(d) Schematic band diagram for metal-STO-domain wall structure and STO–n-type STO 2DEG-domain wall structure. E_{im} indicates impurity bands and E_{dm} indicates domain wall bands. In ferroic domain walls, either impurity bands (semiconducting) or domain wall bands (metallic) could exist, or both of them coexist. (e),(f) Electrical images taken for n-type STO samples with differently orientated conducting domain walls at 5 K.

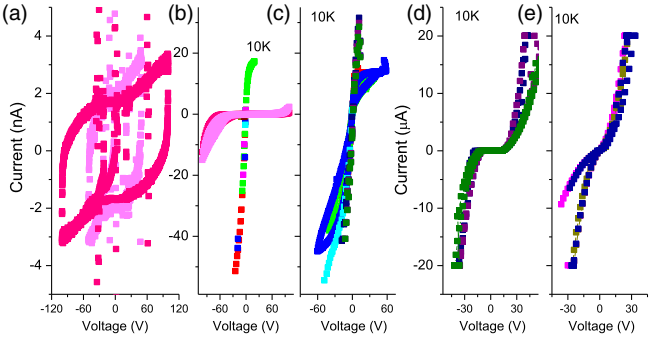

FIG. 2. Different types of current-voltage (IV) curves in insulating bulk STO. (a) Symmetric IV hysteresis loops of insulating bulk STO with gold electrodes as shown in Fig. 1(a). (b) Nonlinear IV curve insulating bulk STO with 2DEG conducting STO electrodes as shown in Fig. 1(b). Enhanced current appears for low temperatures at 10 K in ferroelastic domain walls (always first scan with big loops) and in ferroelectric domain walls (when one decreases gate voltages in the first scan or afterwards with small loops.) comparing to thermal tunneling current at 120 K. (c) IV curves with nonlinearity and hysteresis loops at 10 K in different scans. (d) Largely enhanced current limited by space charge above threshold voltage. (e) Space charge limited current after large voltage scans.

is conducting n-type STO microbridge at the interface of the substrates by growing a few unit cells $LaAlO_3$(LAO) using pulsed laser deposition in (001)-orientated substrates, forming a 2D-electron gas (2DEG) layer [Fig. 1(b)]. Ferroelastic domains were imaged using low-temperature scanning electron microscopy, as described previously in Ref. [10]. Controlled ferroelectric domain walls were created and induced using side gate injection by applying a dc voltage to the microbridge [Figs. 1(e), 1(f)]. Leakage current through domain walls is simultaneously measured with applied voltage as shown in Figs. 1(a), 1(b).

We show the transport measurement of the microbridge and current through the domain walls in Fig. 2. Different types of current I vs voltage V characteristic behaviors have been observed in different samples and measurements. The first type of current-voltage (IV) characteristic is shown in Fig. 2(a) with symmetric hysteresis loops by applying voltage forward and backward (from zero to a maximum voltage $+/-V_m$, then to $-/+V_m$). The maximum current is about a few nA. This IV behavior arises in samples with geometry shown in Fig. 1(a) with gold electrodes. The second (pink solid line) and third (green dot line) types of IV characteristic are shown in Fig. 2(b). The sample with conducting STO 2DEG layer electrodes was cooled down from 120 to 10 K. One important result is the occurrence of electrical conduction at domain walls indicated by a significantly enhanced current of about 20 nA by over 2 orders of magnitude at 10 K comparing to original leakage current at 120 K [10]. The first IV scan at 120 K is just a flat line with a current at ~0.1 nA, as shown in Fig. 3(a). The current loop is reproducible; thus, the enhanced current is not due to breakdown of the device. This current loop is like the dynamic behavior of conductance in domain walls in $BiFeO_3$, indicating a general conductance property of domain walls [12]. Note it is important to measure IV curves in both the forward and reverse directions. As can be seen in Fig. 2, these two curves are asymmetric, indicating the presence of a built-in voltage. The third type of IV curves shown in Fig. 2(b) (pink line) and Fig. 2(d) first scan in the intermediate voltage are similar. In Figs. 2(c)–2(e), the current loops evolve with large current at certain voltage scans above a voltage threshold of ~16 V. At first scans, the current goes to 40 nA, then after several scans the current is significantly enhanced by 4 orders of magnitude and goes to 20 μA, which is limited by our current source. This current I scaled as quadric V^2 is limited by space charges.

In order to study the conduction mechanism in domain walls, we perform current-voltage (IV) characteristic analysis in Fig. 3. Now we focus on the data shown in Figs. 2(b), 2(c). Figure 3(a) shows IV curves at 10 K. It is clear that the current is 1–2 orders of magnitude higher than that of 120 K. Obviously, the current increases fast with voltage and saturates at larger field, as shown in Figs. 3(a), 3(c). The IV curves show resistive switching hysteresis with different scan directions indicated by arrows. The conductance—the slope of the IV curves—decreases with voltage, leading to a negative differential conductance (NDC) (shown in Fig. 4) [13]. Figure 3(d) shows the

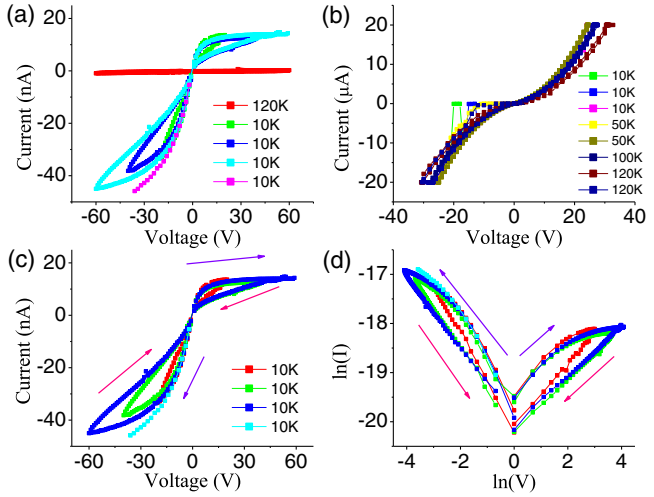

FIG. 3. IV characteristic behavior in STO single crystal with hysteresis and resistive switching. (a) IV curves at 10 K after cooling down from room temperature and 120 K. (b) IV curves showing space charge limited current after several scans at 10 K, and then followed scans at 50, 100, and 120 K. (c) Detailed IV scans at 10 K with directions indicated by arrows. (d) Log-log plot of IV curves shown in (c).

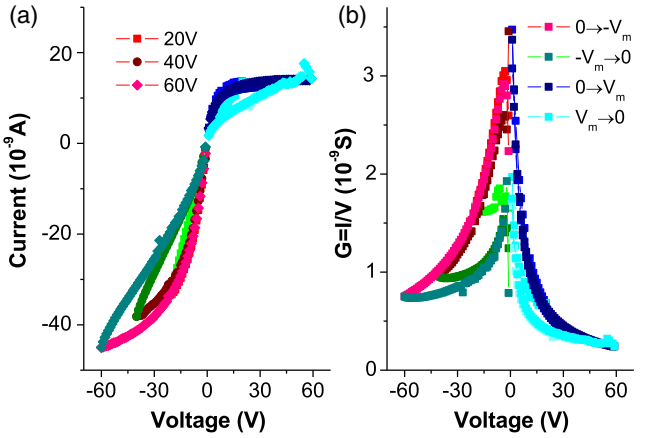

FIG. 4. Negative differential conductance. (a) IV curves. (b) Conductance $G = I/V$ as a function of voltage with slope $dG/dV < 0$ indicating negative differential conductance.

log-log plot of IV curves showing that the scans from large voltages $+/-V_m$ to zero voltage give a linear plot while scans voltage from zero to $+/-V_m$ gives a nonlinear plot indicating non-Ohmic conduction. The linear plot gives exponents of 0.5 and 0.75. Detailed analysis shown in Fig. S1 in the Supplemental Material [14] and below indicates that the conduction mechanism in domain walls showing NDC could not be typical electrode or interface limited mechanisms including Fowler-Nordheim tunneling current [Fig. S1(b)], Schottky emission [Fig. S1 (c)], Richardson-Schottky-Simmons, or Poole-Frenkel (PF) emission [Fig. S1(d)]. In contrast to the electrode or interface limited conduction mechanism of domain walls in ferroelectric $BiFeO_3$ and PZT, the conduction mechanism of domain walls in our samples is shown to be bulk limited.

The bulk-limited conduction mechanisms including Ohmic conduction, Poole-Frenkel emission, hopping conduction, space-charge-limited conduction, ionic conduction, and grain-boundary-limited conduction [15] depend on the electrical properties of the ferroic itself. The most important parameter in this type of conduction mechanism is the trap energy level which could be extracted from conduction data. One could easily exclude Ohmic conduction (linear J vs E), ionic conduction [$J \sim \exp(-E/E_0)$], and grain-boundary-limited conduction (grain boundary in a high resistive state with grains in a low resistive state) for our system. PF is also shown not to be dominant for NDC [Fig. S1(d)]. Thus, the observed non-Ohmic conduction is due to variable range hopping conduction.

In the Ohmic regime, conductivity follows $\sigma \sim \exp[-(T^*/T)^{1/\nu}]$, where $1/\nu$ is $1/(1+d)$ for Mott hopping and $1/2$ for Efros–Shklovskii hopping, d is dimensionality, and T^* is the effective temperature [16–18]. However, it has been demonstrated that the charge transport of low dimensional conductors at low temperatures dominated by variable-range hopping with the influence of Coulomb interactions is unique in the non-Ohmic regime with intermediate electric field $V > k_B T/e$ regardless of the resistivity of samples [19]. In this case, the electric field dependent current follows $I = I_0 \exp[-(E_0/E)^{1/s}]$. It has been shown that $1/s$ equals to $1/(1+d)$ for systems without Coulomb gap and low density amorphous semiconductors where the Coulomb gap plays no role [19–21]. In the presence of the Coulomb gap, $1/s$ is $1/2$ for all dimensions [22]. It was understood that if Ohmic conductivity obeys Efros-Shklovskii law $\exp[-(T_{\rm ES}/T)^{1/2}]$, the electric field dependence of current should be similar with effective temperature $T_{\rm eff} = eEa/k_B$ where a is localization length [22]. In our case, it is almost fully in the non-Ohmic regime for the whole voltage range we measure as $V_c = k_B T/e$ is about 1 mV at 10 K (Figs. 4 and 5); thus, the electric field exponent is the most reliable way to distinguish Mott and Shklovskii hopping. We show current I vs $V^{-1/2}$ in Fig. 5, it is clear that current scales perfectly as $I \sim \exp[-(V^*/V)^{-1/2}]$, where V^* is the effective voltage parameter. This indicates that the mechanism of the observed conduction is Shklovskii variable range hopping with the presence of a Coulomb gap [23,24] (Fig. S2 in the Supplemental Material [14] shows a plot of I as a function of $V^{-1/s}$ with $1/s$ being $1/2$, $1/3$, and $1/4$).

As shown in Figs. 2(d), 2(e), and 3(b), we observe space charge limited current (SCLC) $I = AV^2$ in insulating STO [Fig. 6(a)], where A is the coefficient [25,26]. The space charge limited current starts to appear when one applies large electric field [Fig. 3(b)]. After applying a few voltage

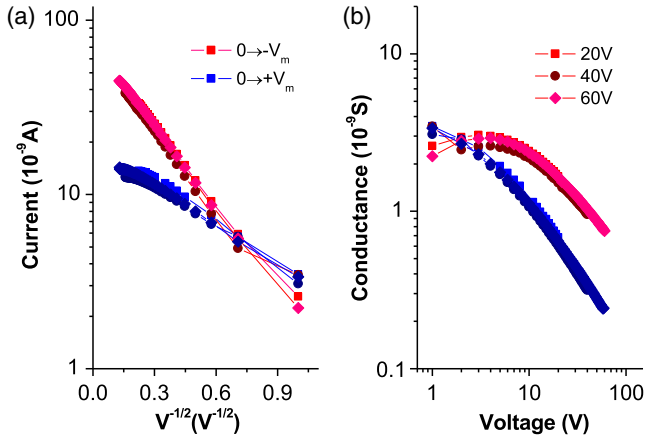

FIG. 5. Shklovskii hopping conduction. (a) Semilog plot of I as a function of $V^{-1/2}$. (b) Conductance as a function of voltage in a log-log plot.

scans, the space charge limited current becomes stable and could even exist when the samples are warmed up to 120 K. The coefficient changes as a function of temperature [Fig. 6(b)], which could be deduced from Mott-Gurney law $I = \frac{9}{8}\theta\mu\varepsilon\varepsilon_r(V^2/L^2)W$ [25–27], where θ is defined as the trap factor, μ is the mobility, L is the distance between the contacts, W is the width of the contacts, ε, ε_r are the dielectric constant for free space and insulator, respectively. In our devices, L and W are about 100 μm. θ is 1 in the case of absence of trapped carriers, otherwise positive but smaller than 1. In the SCLC regime, the current is dominated by charge carriers injected from the contacts, depending only on the mobility; hence, the mobility can be estimated from IV data. Taking ε_r of 18 000 at 10 K and 1000 at 120 K for STO [28], and ε of 8.85×10^{-12} F/m, we could extract the charge mobility limit in the range of 17 and 210 cm^2/Vs. This is in clear contrast to the mobility of

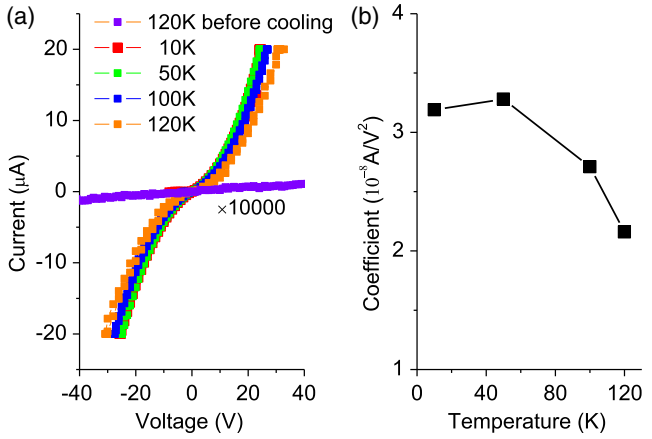

FIG. 6. Space charge limited currents at domain walls. (a) IV curves showing space charge limited currents at different temperatures of 10, 50, 100 and 120 K. (b) Extracted coefficient of IV curves ($I = A_{\text{coeff}}V^2$) at different temperatures.

~1000 cm^2/Vs in 2DEG [11] or even 20 000 cm^2/Vs in artificial nanowires in 2DEG built on STO [29]. As SCLC is not actually a single physical mechanism, it generally includes contributions from Schottky, Poole-Frenkel, and Shklovskii hopping, and it is a condition or threshold for behavior when all of these contributions reach a certain magnitude. Thus, the mobility extracted from SCLC in domain walls in insulating STO is totally different from the mobility obtained in the Ohmic regime in doped STO with the presence of metallic high mobility domain walls [10,24,30]. The presence of disorder and impurity trap centers leading to non-Ohmic variable range hopping is unfavored for high mobility observed in 2DEG or nanowires created on 2DEG.

Both the geometrical traps with random disorder and the Coulomb blockade can cause NDC, but there seems to be no simple way to obtain memory effects in the model of geometrical traps. In the Coulomb blockade picture, however, memory effects seem possible in principle. One of the key elements of the Shklovskii model is that it requires some disorder. In STO, oxygen vacancies, Sr-disorder along the [111] direction (Fig. S3 [14]), and disorder due to point defects could be present [31]. The microscopic picture in the Shklovskii hopping is that the transport of an electron will be determined by sites that are hard to escape due to the high electric field. These sites are those that have no close neighbors in the transport direction, so that to leave one of them the electron either has to make a long jump in the transport direction or return against the field. In Shklovskii hopping in low density random potentials [13,32,33], electrons in trapping centers dominate conduction when the electric field goes against zero towards either $+/-V_m$; thus the "easy" escape route goes against the electric field, while the "easy" escape route becomes along the electric field when the field goes towards zero and the NDC disappears [Fig. 4(b)]. This could be possible in the presence of polar domain walls as the tail to tail polarization forms easy routes for hopping. In intermediate and large electric fields, hopping conduction strongly depends on the trapping of electrons in impurity bands and the conductivity could saturate at certain density with electric field. The resistive switching behavior could also be possible if the trapped states change with electric field [12,34]. The observed [1-11] and [1-1-1] domain walls shown in Fig. S3 [14] indicate the possibility of the presence of the triclinic structure of low-T STO initially determined by NMR spectra [6]. This weakens theories that the superconducting mechanism at low T in STO is based on an antiferroelectric tetragonal distortion at 105 K. These triclinic domains arise from Sr-ion distortions along [111] axes to a maximum of 20 pm.

In summary, our results show that domain walls in STO show unusual electronic transport behavior that is absolutely different from that in the bulk of the material or in conventional ferroelectric materials. Negative differential

conductance is observed with an *IV* hysteresis loop due to the non-Ohmic variable range hopping conduction in domain walls. The conduction mechanism of domain walls is further shown to be Shklovskii hopping in the presence of a Coulomb interaction, which is related to disorder in STO. By analyzing the space charge limited current, we could get the lowest limit of the charge mobility. This work provides direct measurement showing that domain walls in STO are conducting, with an unusual Shklovskii hopping conduction.

We thank the National Science Foundation (NSF) of China No. 61904140 for financial support. H. J. H. Ma acknowledges B. I. Shklovskii for helpful discussions and M. Lange for help with the measurements.

*To whom correspondence should be addressed.
mahj07@xidian.edu.cn
†To whom correspondence should be addressed.
jfs4@st-andrews.ac.uk

[1] J. Seidel *et al.*, Conduction at domain walls in oxide multiferroics. Nat. Mater. **8**, 229 (2009).
[2] G. Catalan, J. Seidel, R. Ramesh, and J. F. Scott, Domain wall nanoelectronics, Rev. Mod. Phys. **84**, 119 (2012).
[3] J. Seidel *et al.*, Domain Wall Conductivity in La-Doped $BiFeO_3$, Phys. Rev. Lett. **105**, 197603 (2010).
[4] S. Farokhipoor and B. Noheda, Conduction through 71° Domain Walls in $BiFeO_3$ Thin Films, Phys. Rev. Lett. **107**, 127601 (2011).
[5] J. Guyonnet, I. Gaponenko, S. Gariglio, and P. Paruch, Conduction at domain walls in insulating $Pb(Zr_{0.2}Ti_{0.8})O_3$ thin films, Adv. Mater. **23**, 5377 (2011).
[6] E. K. H. Salje, O. Aktas, M. A. Carpenter, V. V. Laguta, and J. F. Scott, Domains within Domains and Walls within Walls: Evidence for Polar Domains in Cryogenic $SrTiO_3$, Phys. Rev. Lett. **111**, 247603 (2013).
[7] J. F. Scott, E. K. H. Salje, and M. A. Carpenter, Domain Wall Damping and Elastic Softening in $SrTiO_3$: Evidence for Polar Twin Walls, Phys. Rev. Lett. **109**, 187601 (2012).
[8] T. Zykova-Timan and E. K. H. Salje, Highly mobile vortex structures inside polar twin boundaries in $SrTiO_3$, Appl. Phys. Lett. **104**, 082907 (2014).
[9] P. A. Fleury, J. F. Scott, and J. M. Worlock, Soft Phonon Modes and the 110°K Phase Transition in $SrTiO_3$, Phys. Rev. Lett. **21**, 16 (1968).
[10] H. J. H. Ma, S. Scharinger, S. W. Zeng, D. Kohlberger, M. Lange, A. Stöhr, X. Renshaw Wang, T. Venkatesan, R. Kleiner, J. F. Scott, J. M. D. Coey, D. Koelle, and Ariando, Local Electrical Imaging of Tetragonal Domains and Field-Induced Ferroelectric Twin Walls in Conducting $SrTiO_3$, Phys. Rev. Lett. **116**, 257601 (2016).
[11] A. Ohtomo and H. Y. Hwang, A high-mobility electron gas at the $LaAlO_3/SrTiO_3$ heterointerface, Nature (London) **427**, 423 (2004).
[12] P. Maksymovych, J. Seidel, Y. H. Chu, P. P. Wu, A. P. Baddorf, L.-Q. Chen, S. V. Kalinin, and R. Ramesh, Dynamic conductivity of ferroelectric domain walls in $BiFeO_3$, Nano Lett. **11**, 1906 (2011).
[13] A. V. Nenashev, F. Jansson, S. D. Baranovskii, R. Österbacka, A. V. Dvurechenskii, and F. Gebhard, Hopping conduction in strong electric fields: Negative differential conductivity, Phys. Rev. B **78**, 165207 (2008).
[14] See Supplemental Material at http://link.aps.org/supplemental/10.1103/PhysRevLett.124.146601 for fittings of the *IV* data to different models, and images of domain walls including conducting stripes along [1-11] and [1-1-1] observed in conducting n-type STO.
[15] F.-C. Chiu, A review on conduction mechanisms in dielectric films, Adv. Mater. Sci. Eng. **2014**, 578168 (2014).
[16] A. L. Efros and B. I. Shklovskii, Coulomb gap and low temperature conductivity of disordered systems, J. Phys. C **8**, L49 (1975).
[17] S. V. Malinin, T. Nattermann, and B. Rosenow, Quantum creep and variable-range hopping of one-dimensional interacting electrons, Phys. Rev. B **70**, 235120 (2004).
[18] H. J. Harsan Ma, P. Yang, Z. S. Lim, and Ariando, Mott variable range hopping and bad-metal in lightly doped spin-orbit Mott insulator $BaIrO_3$, Phys. Rev. Mater. **2**, 065003 (2018).
[19] M. M. Fogler and R. S. Kelley. Non-Ohmic Variable-Range Hopping Transport in One-Dimensional Conductors, Phys. Rev. Lett. **95**, 166604 (2005).
[20] B. I. Shklovskii, Hopping conduction in semiconductors subjected to a strong electric field, Fiz. Tekh. Poluprovodn. (S.-Peterburg) **6**, 2335 (1972) [Sov. Phys. Semicond. **6**, 1964 (1973)].
[21] A. N. Aleshin, J. Y. Lee, S. W. Chu, S. W. Lee, B. Kim, S. J. Ahn, and Y. W. Park, Hopping conduction in polydiacetylene single crystals, Phys. Rev. B **69**, 214203 (2004).
[22] S. Marianer and B. I. Shklovskii, Effective temperature of hopping electrons in a strong electric field, Phys. Rev. B **46**, 13100 (1992).
[23] T. Nattermann, T. Giamarchi, and P. Le Doussal, Variable-Range Hopping and Quantum Creep in One Dimension, Phys. Rev. Lett. **91**, 056603 (2003).
[24] B. Kalisky *et al.*, Locally enhanced conductivity due to the tetragonal domain structure in $LaAlO_3/SrTiO_3$ heterointerfaces, Nat. Mater. **12**, 1091 (2013).
[25] O. Marinov, M. J. Deen, and R. Datars, Compact modeling of charge carrier mobility in organic thin-film transistors, J. Appl. Phys. **106**, 064501 (2009).
[26] J. A. Geurst, Theory of space-charge-limited currents in thin semiconductor layers, Physica Status Solidi (b) **15**, 107 (1966).
[27] M. A. Lampert, Volume-controlled current injection in insulators, Rep. Prog. Phys. **27**, 329 (1964).
[28] H. E. Weaver, Dielectric properties of single crystals of $SrTiO_3$ at low temperatures, J. Phys. Chem. Solids **11**, 274 (1959).
[29] P. Irvin, J. P. Veazey, G. Cheng, S. Lu, C.-W. Bark, S. Ryu, C.-B. Eom, and J. Levy, Anomalous high mobility in $LaAlO_3/SrTiO_3$ nanowires, Nano Lett. **13**, 364 (2013).
[30] Cheng *et al.*, Anomalous Transport in Sketched Nanostructures at the $LaAlO_3/SrTiO_3$ Interface, Phys. Rev. X **3**, 011021 (2013).

[31] R. Blinc, B. Zalar, V. V. Laguta, and M. Itoh, Order-Disorder Component in the Phase Transition Mechanism of ^{18}O Enriched Strontium Titanate, Phys. Rev. Lett. **94**, 147601 (2005).

[32] E. I. Levin and B. I. Shklovskii, Negative differential conductivity of low density electron gas in random potential, Solid State Commun. **67**, 233 (1988).

[33] N. van Lien and B. I. Shklovskii, Hopping conduction in strong electric fields and directed percolation, Solid State Commun. **38**, 99 (1981).

[34] R. K. Vasudevan, Y. Cao, N. Laanait, A. Ievlev, L. L. Li, J.-C. Yang, Y.-H. Chu, L.-Q. Chen, S. V. Kalinin, and P. Maksymovych, Field enhancement of electronic conductance at ferroelectric domain walls, Nat. Commun. **8**, 1318 (2017).